

Gapless spin-excitations in the superconducting state of a quasi-one-dimensional spin-triplet superconductor

Keith M. Taddei,^{1,*} Bing-Hua Lei,² Michael A. Susner,³ Hui-Fei Zhai,⁴ Thomas J. Bullard,^{5,6} Liurukara D. Sanjeewa,⁷ Qiang Zheng,⁷ Athena S. Sefat,⁷ Songxue Chi,¹ Clarina dela Cruz,¹ David J. Singh,^{2,†} and Bing Lv^{4,‡}

¹*Neutron Scattering Division, Oak Ridge National Laboratory, Oak Ridge, TN, 37831, USA*

²*Department of Physics and Astronomy, University of Missouri, Missouri 65211, USA*

³*Materials and Manufacturing Directorate, Air Force Research Laboratory,*

Wright-Patterson Air Force Base, OH, 45433, USA

⁴*University of Dallas, Richardson, TX, USA*

⁵*Aerospace Systems Directorate, Air Force Research Laboratory,*

Wright-Patterson Air Force Base, OH, 45433 USA

⁶*UES, Inc., 4401 Dayton Xenia Road, Dayton, Ohio, 45432, USA*

⁷*Materials Science Division, Oak Ridge National Laboratory, Oak Ridge, TN, 37831, USA*

(Dated: June 24, 2022)

Majorana zero modes form as intrinsic defects in an odd-orbital one-dimensional superconductor thus motivating the search for such materials in the pursuit of Majorana physics. Here, we present combined experimental results and first principles calculations which suggest that quasi-one-dimensional $\text{K}_2\text{Cr}_3\text{As}_3$ may be such a superconductor. Using inelastic neutron scattering we probe the dynamic spin-susceptibilities of $\text{K}_2\text{Cr}_3\text{As}_3$ and $\text{K}_2\text{Mo}_3\text{As}_3$ and show the presence of antiferromagnetic spin-fluctuations in both compounds. Below the superconducting transition, these fluctuations gap in $\text{K}_2\text{Mo}_3\text{As}_3$ but not in $\text{K}_2\text{Cr}_3\text{As}_3$. Using first principles calculations, we show that these fluctuations likely arise from nesting on one dimensional features of the Fermi surface. Considering these results we propose that while $\text{K}_2\text{Mo}_3\text{As}_3$ is a conventional superconductor, $\text{K}_2\text{Cr}_3\text{As}_3$ is likely a spin-triplet, and consequently, topological superconductor.

To realize scaleable quantum computers, new phenomena on which to base the qubit are needed - ones robust and with intrinsic entangled properties such as exists in certain topological phases [1–9]. Of the potential candidates, the Majorana zero mode (MZM) is one of the most promising due to its non-abelian anyon statistics which are suited for braiding while also potentially allowing for physical manipulation as is necessary for computation [10–15]. However, generating and observing MZMs has proven challenging with several potential routes in active pursuit such as: at the interface of a topological insulator and a superconductor (SC), in a SC with a topological band structure, or in a SC whose pair operator is its own conjugate - a ‘spin-less’ or spin-triplet odd-orbital SC [16]. Indeed, this last case (when restricted to one dimension) is related to the toy-model first proposed by Kitaev to generate physically separated MZM [11].

As a result, there is great interest in one-dimensional (1D) or quasi-1D (Q1D) systems which might exhibit spin-triplet SC (TSC) - especially those that exhibit both properties intrinsically. However, such materials are extraordinarily rare with few compounds showing either property and still fewer with both. Nonetheless, several candidate materials have been found (including the Bechgaard salts, purple bronze, and even possibly Sr_2RuO_4) [17–19]. More recently, the discovery of the Q1D potential TSC $A_n\text{H}_{(2-n)x}\text{TM}_3\text{As}_3$ (with $A = \text{Na, K, Rb or Cs}$, $\text{TM} = \text{Cr or Mo}$ and $n = 1$ or 2) family has provided another route to realize these exotic physics [20–29].

The $A_n\text{H}_{(2-n)x}\text{TM}_3\text{As}_3$ materials exhibit numerous

novel properties, several of which evince TSC. These materials crystallize with a Q1D structural motif of TM_3As_3 tubes which give rise to strongly Q1D features such as Luttinger-liquid physics, Q1D Fermi surfaces (FS) and highly anisotropic transport [20, 21, 27, 30–33]. Enticingly, their SC state appears to be unconventional with an unexpectedly high upper critical field, potential nodes in the SC gap, and a proximity to a quantum critical point with possible suggestions of TSC due to a spontaneous magnetization below the SC transition (T_C), an angular dependent upper critical field, ferromagnetic (FM) fluctuations, a T_C suppressed by non-magnetic impurities and widespread findings of a leading TSC instability from theory [34–46].

However, the symmetry of the SC state, and thus the prospects for hosting MZM, remains disputed. While some studies support TSC, others have suggested a spin-singlet state. These investigations report anti-FM (AFM) instabilities, a proximity to a spin-glass state, a s^\pm gap symmetry, and even claims of standard electron-phonon (e - p) coupling [29, 47–49]. Recently, it was proposed that the $\text{K}_2\text{TM}_3\text{As}_3$ family may straddle a boundary between an unconventional SC in $\text{K}_2\text{Cr}_3\text{As}_3$ ($T_C \sim 6$ K) and a multi-gap conventional SC in $\text{K}_2\text{Mo}_3\text{As}_3$ ($T_C \sim 10$ K), perhaps giving some guidance to understand the disparate reported features [50].

In this Letter, we assess the possibility of TSC in $\text{K}_2\text{Cr}_3\text{As}_3$ through a careful study of the dynamic spin susceptibilities of $\text{K}_2\text{Cr}_3\text{As}_3$ and $\text{K}_2\text{Mo}_3\text{As}_3$ using both experimental probes and first principles calculations. To start, inelastic neutron scattering (INS) experiments re-

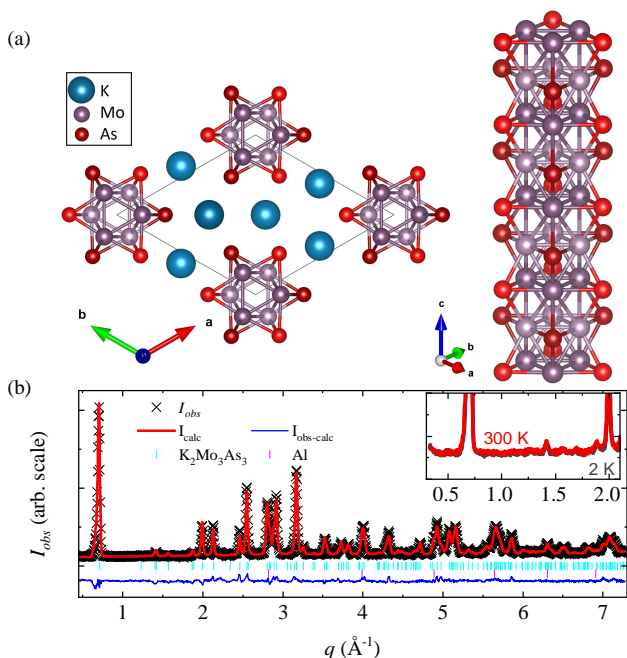


FIG. 1. (a) Crystal structure of $K_2Mo_3As_3$ viewed along c and of the isolated tube motif. (b) Neutron powder diffraction pattern and best model fit for data collected at 300 K. Inset of panel (b) shows a comparison of the low q region of data collected at 300 and 2 K.

veal spin-fluctuations (SF) in both compounds above T_C which are consistent with an incipient AFM order. Below T_C , we find that for $K_2Mo_3As_3$ a resonanceless spin-gap opens while in $K_2Cr_3As_3$ no gap is observed implying a difference in the compounds' SC states. Performing first principles calculations, we find that the AFM SF can be explained by FS nesting on one dimensional FSs. Consequently, we suggest that $K_2Mo_3As_3$ is an e - p SC whose low energy SF are suppressed due to the opening of SC gaps on all FSs. Contrastingly, the lack of a spin-gap in $K_2Cr_3As_3$ indicates that neither the AFM SF nor the associated FSs participate in SC leaving a single remaining FS which much be SC and is favorable to FM SF driven TSC. These conclusions support the scenario of FM driven TSC in $K_2Cr_3As_3$ and indicate its potential for hosting topological SC.

Large powder samples of $K_2Cr_3As_3$ and $K_2Mo_3As_3$ were synthesized using methods reported previously to obtain ~ 10 g of materials per compound (see the supplemental materials (SM) for details) [20, 27, 47]. Neutron powder diffraction (NPD) measurements were performed on the HB-2A diffractometer of Oak Ridge National Laboratory's (ORNL) High Flux Isotope Reactor (HFIR) [51]. The resulting diffraction data were analyzed using the Rietveld method as implemented in the FullProf software Suite [52]. INS was performed on the HB-3 and CTAX triple axis spectrometers of HFIR using fixed analyzer energies of 14.7 and 5 meV respectively.

To calculate the electronic band structure, Density Functional Theory (DFT) calculations were performed using the generalized gradient approximation of Perdew, Burke and Ernzerhof (PBE) and the general potential linearized augmented planewave method as implemented in the WIEN2k code [53–55].

In fig. 1 (a) we show the crystal structure of $K_2Mo_3As_3$ (space group $P6m2$) which exhibits a unique Q1D structural motif comprised of two inequivalent, alternating, coaxial layers of Mo (and As) triangles. In fig. 1(b) we show a diffraction pattern of $K_2Mo_3As_3$ collected at 300 K together with a simulated pattern from our best-fit model (we note that we found no impurity phase in our diffraction data indicating the high quality of our sample). In the inset of fig. 1(b) we show a comparison of NPD patterns collected at 300 and 2 K demonstrating a lack of any significant changes which might be associated with the onset of magnetic order indicating that $K_2Mo_3As_3$ (as $K_2Cr_3As_3$) has no long-range magnetic order (see the SM for more discussion) [56].

Previously, $K_2Cr_3As_3$ was shown to have AFM SF arising from incipient $\mathbf{k} = (0, 0, \frac{1}{2})$ type order. This was revealed as a column of scattering in the dynamic structure factor $S(q, \Delta E)$ (as probed via INS) which is proportional to the imaginary component of the spin-susceptibility [47, 57, 58]. Such fluctuations and their temperature dependence offer significant insights to the SC state. Therefore, we now turn to similar experiments performed on $K_2Mo_3As_3$ and expand on our previous work on $K_2Cr_3As_3$ to compare their respective $S(q, \Delta E)$.

Fig. 2(a) and (c) show the $S(q, \Delta E)$ of $K_2Mo_3As_3$ and $K_2Cr_3As_3$ collected at 20 and 10 K respectively (i.e. above either compound's T_C). Here we focus on the low q and low ΔE region which is typically featureless at these temperatures for non-magnetic materials. However, for both materials a column of scattering is seen arising from $\sim 0.75 \text{ \AA}^{-1}$. Such a signal is often indicative of incipient magnetic order caused by SF with a q characteristic of the incipient ordering vector [40, 58–62].

Qualitatively, the signal observed in $K_2Mo_3As_3$ is similar to that of $K_2Cr_3As_3$. Fitting the constant ΔE cuts of the two datasets with Gaussian functions, we find a slight shift in the position of the feature to lower q by $\sim 0.1 \text{ \AA}^{-1}$ in $K_2Mo_3As_3$ compared to $K_2Cr_3As_3$ which is consistent with the larger c axis (see SM for details) [56]. Furthermore, the dispersion of the two signals is very similar (albeit they are both skewed due to the instrument's resolution function). On the other hand, the fits reveal that the column in $K_2Mo_3As_3$ is broader in q by $\sim 20\%$ and also is $\sim 30\%$ weaker (though this is more difficult to reliably quantify between samples) which may indicate the fluctuations are shorter-ranged and a smaller fluctuating moment is present in $K_2Mo_3As_3$ - both of which have been suggested from prior DFT treatments [50]. Due to these considerations, we attribute the origin of this signal to similar causes as in $K_2Cr_3As_3$.

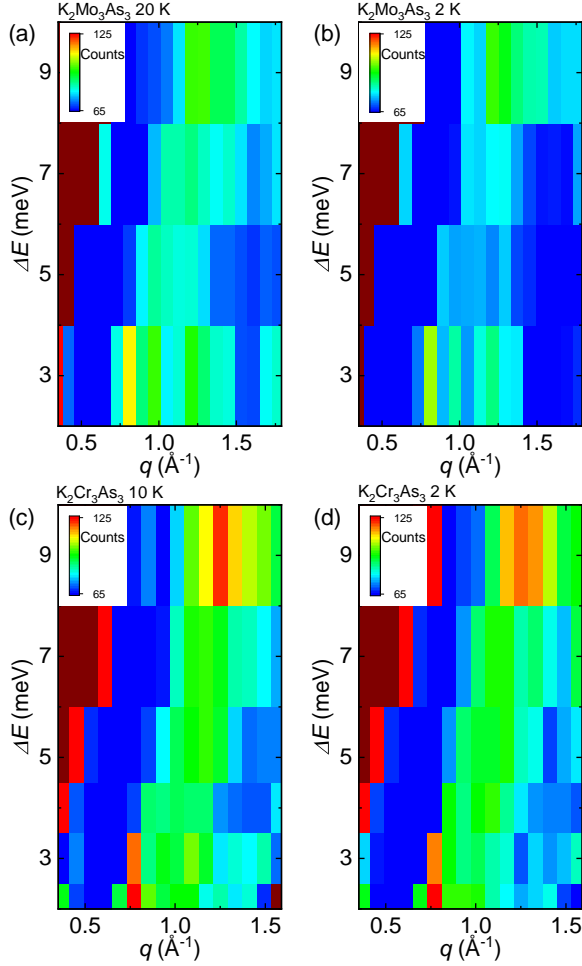


FIG. 2. Inelastic neutron scattering spectrograms for $\text{K}_2\text{Mo}_3\text{As}_3$ at (a) 20 K and (b) 2 K and for $\text{K}_2\text{Cr}_3\text{As}_3$ at (c) 10 K and (d) 2 K. Intensity is in units of detector counts normalized to monitor counts. We note that the data showed in panel (c) includes data from ref. 47 but with additional counting statistics.

With the origin identified, we now turn to the temperature dependencies across T_C . Fig. 2(b) and (d) show the same region of $S(q, \Delta E)$ measured below T_C at 2 K for both samples. Here a distinction between the two emerges. For $\text{K}_2\text{Cr}_3\text{As}_3$ the spectrograph looks qualitatively identical to the 20 K data set. In particular, no gap opens in the fluctuations despite the onset of SC. On the other hand, in $\text{K}_2\text{Mo}_3\text{As}_3$ (fig. 2(b)) there is a clear change in the column where the signal for $\Delta E < 7$ meV loses intensity. This observation is consistent with the opening of a SC gap which inhibits fluctuations below 2Δ (i.e. the energy required to break a Cooper pair).

To characterize this feature more carefully, constant q scans were taken at $q \sim 1.1 \text{ \AA}^{-1}$ above and below T_C for both samples (fig. 3). For $\text{K}_2\text{Mo}_3\text{As}_3$ (fig. 3(a)), the gap becomes clear. While the 20 K data exhibit a con-

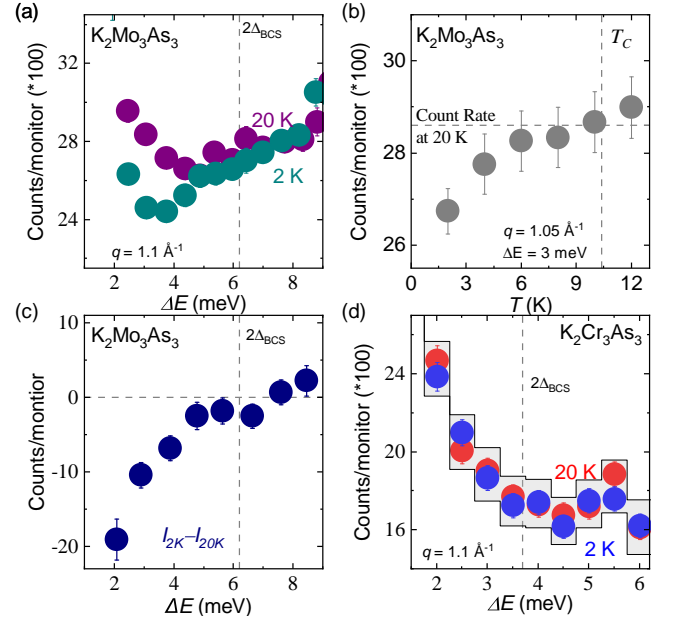


FIG. 3. (a) Comparison of scattering intensity of $\text{K}_2\text{Mo}_3\text{As}_3$ for constant q scans along the column collected at 20 and 2 K. (b) Temperature dependence of the low energy region of the $\text{K}_2\text{Mo}_3\text{As}_3$ column with the 20 K count rate and T_C denoted by horizontal and vertical dotted lines. (c) Difference curve for the 20 and 2 K scans of $\text{K}_2\text{Mo}_3\text{As}_3$ shown in panel (a). (d) Similar comparison of 20 K and 2 K scans for $\text{K}_2\text{Cr}_3\text{As}_3$ with the an envelope denoting the size of a gap expected for a signal similar to that observed in panel (a).

stant increase in intensity below 5 meV (as the elastic line is approached), the 2 K data exhibit a qualitatively different behavior, dropping in intensity by $\sim 20\%$ below ~ 5 meV. Using the weak coupling Bardeen Cooper Schieffer gap approximation (i.e. $\Delta(T = 0) = \frac{7}{2}k_B T_C$) we estimate 2Δ as 6.2 meV which is consistent with our observed gap (a similar estimate is obtained using the empirical formula of $\omega_0 = 4.3k_B T_c$ with ω_0 being the energy of the spin-gap in the SC state)[63]. In fig. 3(c) we show a difference curve between the 20 and 2 K data to remove background effects. Here, the gap is seen to open below ~ 5 meV and progressively widen to the lowest measured temperature of 2 K. We note that the shape of this curve may corroborate nodal or nodeless gap functions however, we do not believe our data are sufficient to allow such an analysis. We further associate this gap with T_C by measuring the intensity at 1.05 \AA^{-1} and 3 meV as a function of temperature (fig. 3(b)) which shows the gap to close at ~ 6 K. This is a little below T_C (10.4 K); however, the gap itself is a function of T and so should become smaller than the certainty of our measurements before T_C is exceeded.

Turning to $\text{K}_2\text{Cr}_3\text{As}_3$, we see discretely different behavior in the low energy spectrum (fig. 3(d)). Here, no obvious gap in the fluctuations is seen in the 2 K data.

If the gap size is estimated as before, $2\Delta \sim 3.7$ meV and $\omega_0 \sim 2.2$ meV, both of which are within the limits of our energy resolution (~ 1 meV). For comparison, in fig. 3(d) we plot an envelope showing the range equivalent to the percent change of the signal seen in $\text{K}_2\text{Mo}_3\text{As}_3$, demonstrating that, within our statistics, a similar decrease in intensity should be observable if present. Additional measurements were taken using a cold neutron triple-axis spectrometer to access lower energy transfers (< 1 meV) and no gap was observed (see SM)[56]. Consequently, we take this observation to be a strong indication that no spin-gap opens in the SC state of $\text{K}_2\text{Cr}_3\text{As}_3$.

Such an observation has significant implications for the nature of SC in these systems as well as how it evolves between the two materials [50]. That the SF in $\text{K}_2\text{Cr}_3\text{As}_3$ do not respond strongly to SC requires an explanation - naively SC should open a gap. Furthermore, though a spin-gap with an accompanying resonance has become a hallmark of unconventional SCs near magnetic order, here we see no evidence of a resonance above the gap in $\text{K}_2\text{Mo}_3\text{As}_3$ and no resonance or gap in $\text{K}_2\text{Cr}_3\text{As}_3$ undermining SF possible role in SC [64]. To help interpret these observations we note that if the SF can be associated with specific features of the FSs then the presence (or absence) of a gap in those SF will directly correspond to the presence (or absence) of a gap on the associated FS. In a system such as $\text{K}_2\text{Cr}_3\text{As}_3$, where different FSs have different SC instabilities, such information can be key in determining the symmetry of the SC state [63, 65–77].

To elucidate the origin of the SF, we consider the FSs of $\text{K}_2\text{Mo}_3\text{As}_3$ and (undistorted) $\text{K}_2\text{Cr}_3\text{As}_3$ (shown in fig. 4 (a) and (b)) as determined by DFT calculations. Here we use undistorted $\text{K}_2\text{Cr}_3\text{As}_3$ due to ambiguity in the exact symmetry of the distorted structure [78, 79]. As reported, these two compounds have similar FSs, consisting of two Q1D α and β sheets and one large 3D γ sheet [41, 44, 50, 80–82]. Given the large sheet-like features of the FSs, nesting vectors have long been proposed as possible between both the upper and lower α and β sheets as well as between the top and bottom surfaces of the γ sheet any of which may lead to spin- or charge-density wave type orders with such a mechanism being proposed for the SF observed in $\text{K}_2\text{Cr}_3\text{As}_3$ [40, 47, 49, 50, 79, 83].

With the potential for FS nesting established, we next calculate the Fermi velocities (v_F) throughout the FSs of both compounds to predict the strength of electron correlations on the different surfaces (as shown in the color scale on fig. 4 (a) and (b)). These calculations reveal two important features: for both compounds the large 3D γ sheet has significantly lower v_F indicating stronger correlated electron physics on this sheet. Additionally, v_F is in general larger in $\text{K}_2\text{Mo}_3\text{As}_3$ suggesting weaker electron correlations. These results suggest both that magnetic interactions should be stronger on the γ sheet and stronger in $\text{K}_2\text{Cr}_3\text{As}_3$ than in $\text{K}_2\text{Mo}_3\text{As}_3$ in general.

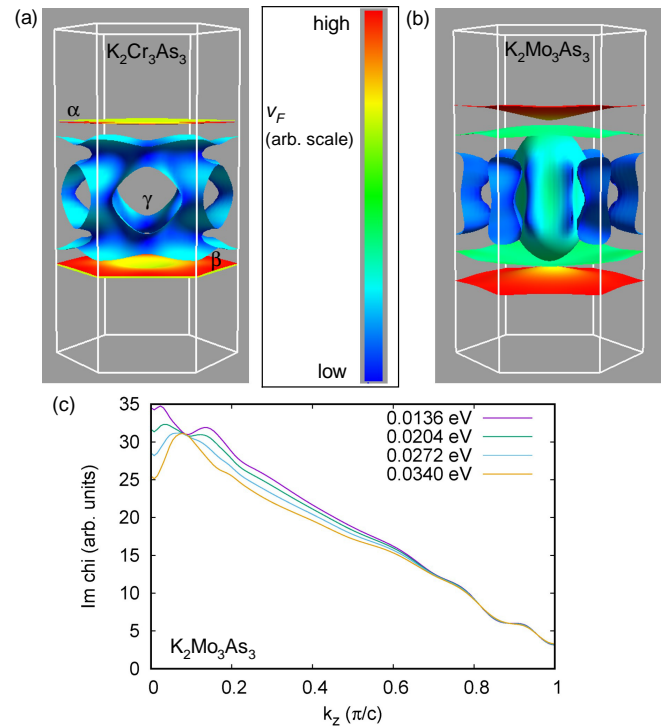


FIG. 4. Calculated Fermi surfaces of (a) $\text{K}_2\text{Cr}_3\text{As}_3$ (undistorted) and (b) $\text{K}_2\text{Mo}_3\text{As}_3$. In (a) and (b) the calculated Fermi velocity is shown as a function of position on the Fermi surface via the color scale with blue indicating low relative velocities and red indicating higher velocities. (c) Imaginary component of the calculated Lindhard susceptibility of $\text{K}_2\text{Mo}_3\text{As}_3$ plotted for several energies near the Fermi energy (with $E_F = 0$ eV).

With the Fermiology indicating potential nesting, we turn to calculations of the imaginary component of the Lindhard susceptibility (which corresponds to the dynamic spin susceptibility) projected along k_z for $\text{K}_2\text{Mo}_3\text{As}_3$ (fig. 4(c)) (for this purpose we used a very dense grid of k -points and the constant matrix element approximation). Peaks in the Lindhard susceptibility have previously been reported in $\text{A}_2\text{Cr}_3\text{As}_3$ and ACr_3As_3 and attributed to SF with a nesting vector along k_z consistent with intra-band scattering [44, 83–85]. Here, we most prominently see a large broad peak near the zone center which corresponds to the FM SF observed in nuclear magnetic resonance measurements [40, 59, 86, 87]. However, at larger k_z , near the zone boundary, we see a second feature at $k_z \sim 0.9$ which closely corresponds to the $\mathbf{k} = (0, 0, \frac{1}{2})$ position for the AFM SF observed in INS. This peak is quite small which is consistent with it arising from nesting between the two high v_F Q1D sheets.

These insights from first principles allow us to better interpret the experimental results. They show that both $\text{K}_2\text{Mo}_3\text{As}_3$ and $\text{K}_2\text{Cr}_3\text{As}_3$ have similar potential nesting vectors involving the 1D FSs consistent with the observed column of SF. That the AFM SF do not gap in $\text{K}_2\text{Cr}_3\text{As}_3$

indicates that neither the AFM SF nor the 1D FSs participate in SC. This is expected as symmetry considerations for AFM SF mediated spin-singlet or spin-triplet SC disallow Cooper pairs between k_z and $-k_z$ states [88, 89]. We can also eliminate AFM SF as a candidate mechanism in $\text{K}_2\text{Mo}_3\text{As}_3$ via the lack of a resonant-spin excitation in the SC state despite the observation of a SC gap [83]. Turning to the upgapped Q1D FSs in $\text{K}_2\text{Cr}_3\text{As}_3$, this implies that SC must exist on the γ sheet. Given the strong FM SF present in $\text{K}_2\text{Cr}_3\text{As}_3$ which are known to gap below T_C this points to an interesting scenario [40]. While AFM SF cannot pair k_z and $-k_z$ states, FM SF do allow pairing of such states for a gap sign change as occurs in p_z -wave orbital symmetry [88]. Furthermore, for FM SF the pairing potential is enhanced for low scattering vectors as found here on the γ surface which encompasses the zone center, consistent with the lower v_F found on this sheet [88]. More generally, that both AFM and FM SF exist in $\text{K}_2\text{Cr}_3\text{As}_3$ but only the latter responds to SC is highly suggestive of TSC. Thus, our results are consistent with a p_z -wave TSC state in $\text{K}_2\text{Cr}_3\text{As}_3$ and encourage further work searching for MZMs, potentially pointing to a system which advantageously exhibits a p_z -wave state that avoids the singlet-triplet mixing, a highly Q1D crystal habit which may help with device design as well as in isolating such states, and predictions of other intrinsic topological band features [83, 90, 91].

In summary, we show that both $\text{K}_2\text{Cr}_3\text{As}_3$ and $\text{K}_2\text{Mo}_3\text{As}_3$ exhibit antiferromagnetic spin fluctuations which are consistent with an incipient $\mathbf{k} = (0, 0, \frac{1}{2})$ ordering vector. Comparing spectra collected above and below their respective T_C s, we find that while $\text{K}_2\text{Mo}_3\text{As}_3$ exhibits a gap, $\text{K}_2\text{Cr}_3\text{As}_3$ exhibits no such gap. Furthermore, despite seeing a gap in $\text{K}_2\text{Mo}_3\text{As}_3$, we observe no evidence of a spin-resonance - the hallmark of spin-driven unconventional superconductivity. Using first principles calculations, we show that these two materials are susceptible to nesting across their Q1D Fermi surfaces consistent with a $\mathbf{k} = (0, 0, \frac{1}{2})$. As we observe no gap in the spin-fluctuations of $\text{K}_2\text{Cr}_3\text{As}_3$, we infer that these Fermi surfaces are not gapped by the superconducting state and that the remaining γ sheet, which should favor spin-triplet pairing, must host superconductivity. Furthermore, we rule out the antiferromagnetic and e - p coupling superconducting mechanisms in $\text{K}_2\text{Cr}_3\text{As}_3$, indicating that ferromagnetic fluctuation driven spin-triplet superconductivity is the likely mechanism. As $\text{K}_2\text{Cr}_3\text{As}_3$ is a Q1D material, its hosting spin-triplet superconductivity should have exciting implications for topological physics invoking aspects of Kitaev's toy model for Majorana zero-modes.

Note: While this manuscript was in preparation another paper was published (ref. 92) which came to similar conclusions via nuclear magnetic resonance measurements performed on a single crystal sample of $\text{K}_2\text{Cr}_3\text{As}_3$. These results and ours are quite complementary with the

Knight shift providing a more direct measurement of the superconducting state and our measurements and analysis approaching the question of superconductivity in the $A_2TM_3As_3$ family more comprehensively.

The authors thank Cristian Batista for helpful conversations pertaining to the significance of the gap in $\text{K}_2\text{Mo}_3\text{As}_3$. The part of the research that was conducted at ORNL's High Flux Isotope Reactor was sponsored by the Scientific User Facilities Division, Office of Basic Energy Sciences, US Department of Energy. The research is partly supported by the U.S. Department of Energy (DOE), Office of Science, Basic Energy Sciences (BES), Materials Science and Engineering Division. Work at the University of Missouri is supported by the U.S. DOE, BES, Award No. DE-SC0019114. The part of this work performed at the University of Texas at Dallas is supported by U.S. Air Force Office of Scientific Research (FA9550-19-1-0037) and National Science Foundation (DMR 1921581). The contribution performed at Air Force Research laboratory was supported by the United States Air Force Office of Scientific Research (AFOSR) LRIR 18RQCOR100 as well as AOARD-MOST Grant Number F4GGA21207H002.

Notice of Copyright This manuscript has been authored by UT-Battelle, LLC under Contract No. DE-AC05-00OR22725 with the U.S. Department of Energy. The United States Government retains and the publisher, by accepting the article for publication, acknowledges that the United States Government retains a non-exclusive, paid-up, irrevocable, world-wide license to publish or reproduce the published form of this manuscript, or allow others to do so, for United States Government purposes. The Department of Energy will provide public access to these results of federally sponsored research in accordance with the DOE Public Access Plan (<http://energy.gov/downloads/doe-public-access-plan>).

* corresponding author taddeikm@ornl.gov

† singhdj@missouri.edu

‡ blv@utdallas.edu

- [1] F. Arute, K. Arya, R. Babbush, D. Bacon, J. C. Bardin, R. Barends, R. Biswas, S. Boixo, F. G. Brandao, D. A. Buell, *et al.*, Quantum supremacy using a programmable superconducting processor, *Nature* **574**, 505 (2019).
- [2] C. Ballance, T. Harty, N. Linke, M. Sepiol, and D. Lucas, High-fidelity quantum logic gates using trapped-ion hyperfine qubits, *Phys. Rev. Lett.* **117**, 060504 (2016).
- [3] M. H. Devoret and R. J. Schoelkopf, Superconducting circuits for quantum information: an outlook, *Science* **339**, 1169 (2013).
- [4] M. R. Geller, E. J. Pritchett, A. T. Sornborger, and F. Wilhelm, Quantum computing with superconductors i: Architectures, in *Manipulating Quantum Coherence in Solid State Systems* (Springer, 2007) pp. 171–194.

- [5] K. D. Petersson, J. R. Petta, H. Lu, and A. C. Gosard, Quantum coherence in a one-electron semiconductor charge qubit, *Phys. Rev. Lett.* **105**, 246804 (2010).
- [6] A. Y. Kitaev, Fault-tolerant quantum computation by anyons, *Ann. Phys.* **303**, 2 (2003).
- [7] C. Nayak, S. H. Simon, A. Stern, M. Freedman, and S. Das Sarma, Non-abelian anyons and topological quantum computation, *Rev. Mod. Phys.* **80**, 1083 (2008).
- [8] A. Stern and N. H. Lindner, Topological quantum computation—from basic concepts to first experiments, *Science* **339**, 1179 (2013).
- [9] N. P. de Leon, K. M. Itoh, D. Kim, K. K. Mehta, T. E. Northup, H. Paik, B. Palmer, N. Samarth, S. Sangtawesin, and D. Steuerman, Materials challenges and opportunities for quantum computing hardware, *Science* **372** (2021).
- [10] C. Beenakker, Search for majorana fermions in superconductors, *Annu. Rev. Condens. Matter Phys.* **4**, 113 (2013).
- [11] A. Y. Kitaev, Unpaired majorana fermions in quantum wires, *Phys.-Uspekhi* **44**, 131 (2001).
- [12] S. Vaitiekėnas, G. Winkler, B. van Heck, T. Karzig, M.-T. Deng, K. Flensberg, L. Glazman, C. Nayak, P. Krogstrup, R. Lutchyn, *et al.*, Flux-induced topological superconductivity in full-shell nanowires, *Science* **367** (2020).
- [13] F.-L. Xiong, H.-L. Lai, and W.-M. Zhang, Manipulating majorana qubit states without braiding, *Phys. Rev. B* **104**, 205417 (2021).
- [14] J. Alicea, Y. Oreg, G. Refael, F. Von Oppen, and M. P. Fisher, Non-abelian statistics and topological quantum information processing in 1d wire networks, *Nat. Phys.* **7**, 412 (2011).
- [15] C. Tutschku, R. W. Reinthaler, C. Lei, A. H. MacDonald, and E. M. Hankiewicz, Majorana-based quantum computing in nanowire devices, *Phys. Rev. B* **102**, 125407 (2020).
- [16] C. Chamon, M. O. Goerbig, R. Moessner, and L. F. Cugliandolo, *Topological Aspects of Condensed Matter Physics: École de Physique Des Houches, Session CIII, 4-29 August 2014*, Vol. 103 (Oxford University Press, 2017).
- [17] S. Brown, Organic superconductors: The bechgaard salts and relatives, *Physica C Supercond.* **514**, 279 (2015).
- [18] W. Cho, C. Platt, R. H. McKenzie, and S. Raghu, Spin-triplet superconductivity in a weak-coupling Hubbard model for the quasi-one-dimensional compound $\text{Li}_{0.9}\text{Mo}_6\text{O}_{17}$, *Phys. Rev. B* **92**, 134514 (2015).
- [19] I. A. Firmo, S. Lederer, C. Lupien, A. P. Mackenzie, J. C. Davis, and S. A. Kivelson, Evidence from tunneling spectroscopy for a quasi-one-dimensional origin of superconductivity in Sr_2RuO_4 , *Phys. Rev. B* **88**, 134521 (2013).
- [20] J.-K. Bao, J.-Y. Liu, C.-W. Ma, Z.-H. Meng, Z.-T. Tang, Y.-L. Sun, H.-F. Zhai, H. Jiang, H. Bai, C.-M. Feng, Z.-A. Xu, and G.-H. Cao, Superconductivity in Quasi-One-Dimensional $\text{K}_2\text{Cr}_3\text{As}_3$, *Physical Review X* **5**, 011013 (2015).
- [21] J.-K. Bao, L. Li, Z.-T. Tang, Y. Liu, Y.-K. Li, H. Bai, C.-M. Feng, Z.-A. Xu, and G.-H. Cao, Cluster spin-glass ground state in quasi-one-dimensional KCr_3As_3 , *Phys. Rev. B* **91**, 180404 (2015).
- [22] J.-J. Xiang, Y.-L. Yu, S.-Q. Wu, B.-Z. Li, Y.-T. Shao, Z.-T. Tang, J.-K. Bao, and G.-H. Cao, Superconductivity induced by aging and annealing in $\text{K}_{1-\delta}\text{Cr}_3\text{As}_3\text{H}_x$, *Phys. Rev. Materials* **3**, 114802 (2019).
- [23] Z.-T. Tang, J.-K. Bao, Y. Liu, Y.-L. Sun, A. Ablimit, H.-F. Zhai, H. Jiang, C.-M. Feng, Z.-A. Xu, and G.-H. Cao, Unconventional superconductivity in quasi-one-dimensional $\text{Rb}_2\text{Cr}_3\text{As}_3$, *Phys. Rev. B* **91**, 020506 (2015).
- [24] Z.-T. Tang, J.-K. Bao, Z. Wang, H. Bai, H. Jiang, Y. Liu, and H.-F. Zhai, Superconductivity in quasi-one-dimensional $\text{Cs}_2\text{Cr}_3\text{As}_3$ with large interchain distance, *Sci. China Mater.* **58**, 16 (2015).
- [25] Z.-T. Tang, J. Bao, Y. Liu, H. Bai, H. Jiang, H.-F. Zhai, C.-M. Feng, Z.-A. Xu, and G.-H. Cao, Synthesis, crystal structure and physical properties of quasi-one-dimensional ACr_3As_3 ($A = \text{Rb}, \text{Cs}$), *Science China Materials* **58**, 543 (2015).
- [26] Q.-G. Mu, B.-B. Ruan, B.-J. Pan, T. Liu, J. Yu, K. Zhao, G.-F. Chen, and Z.-A. Ren, Ion-exchange synthesis and superconductivity at 8.6 K of $\text{Na}_2\text{Cr}_3\text{As}_3$ with quasi-one-dimensional crystal structure, *Phys. Rev. Materials* **2**, 034803 (2018).
- [27] Q.-G. Mu, B.-B. Ruan, K. Zhao, B.-J. Pan, T. Liu, L. Shan, G.-F. Chen, and Z.-A. Ren, Superconductivity at 10.4 K in a novel quasi-one-dimensional ternary molybdenum pnictide $\text{K}_2\text{Mo}_3\text{As}_3$, *Sci. Bull.* **63**, 952 (2018).
- [28] T. Liu, Q.-G. Mu, B.-J. Pan, J. Yu, B.-B. Ruan, K. Zhao, G.-F. Chen, and Z.-A. Ren, Superconductivity at 7.3 K in the 133-type Cr-based RbCr_3As_3 single crystals, *EPL* **120**, 27006 (2017).
- [29] K. M. Taddei, L. D. Sanjeewa, B.-H. Lei, Y. Fu, Q. Zheng, D. J. Singh, A. S. Sefat, and C. dela Cruz, Tuning from frustrated magnetism to superconductivity in quasi-one-dimensional KCr_3As_3 through hydrogen doping, *Phys. Rev. B* **100**, 220503 (2019).
- [30] G. Cao, J.-K. Bao, Z.-T. Tang, Y. Liu, and H. Jiang, Peculiar properties of -chain-based superconductors, *Philos. Mag.* **97**, 591 (2017).
- [31] Q.-G. Mu, B.-B. Ruan, B.-J. Pan, T. Liu, J. Yu, K. Zhao, G.-F. Chen, and Z.-A. Ren, Superconductivity at 5 K in quasi-one-dimensional Cr-based KCr_3As_3 single crystals, *Phys. Rev. B* **96**, 140504 (2017).
- [32] C. Noce, The chromium pnictide materials: A tunable platform for exploring new exciting phenomena, *EPL* **130**, 67001 (2020).
- [33] M. D. Watson, Y. Feng, C. W. Nicholson, C. Monney, J. M. Riley, H. Iwasawa, K. Refson, V. Sacksteder, D. T. Adroja, J. Zhao, and M. Hoesch, Multi-band One-Dimensional Electronic Structure and Spectroscopic Signature of Tomonaga-Luttinger Liquid Behavior in $\text{K}_2\text{Cr}_3\text{As}_3$, *Phys. Rev. Lett.* **118**, 097002 (2017).
- [34] F. F. Balakirev, T. Kong, M. Jaime, R. D. McDonald, C. H. Mielke, A. Gurevich, P. C. Canfield, and S. L. Bud'ko, Anisotropy reversal of the upper critical field at low temperatures and spin-locked superconductivity in $\text{K}_2\text{Cr}_3\text{As}_3$, *Phys. Rev. B* **91**, 220505 (2015), 1505.05547 [cond-mat.supr-con].
- [35] G. M. Pang, M. Smidman, W. B. Jiang, J. K. Bao, Z. F. Weng, Y. F. Wang, L. Jiao, J. L. Zhang, G. H. Cao, and H. Q. Yuan, Evidence for nodal superconductivity in quasi-one-dimensional $\text{K}_2\text{Cr}_3\text{As}_3$, *Phys. Rev. B* **91**, 220502 (2015).
- [36] J. Luo, J. Yang, R. Zhou, Q. G. Mu, T. Liu, Z.-a. Ren, C. J. Yi, Y. G. Shi, and G.-q. Zheng, Tuning the Distance to a Possible Ferromagnetic Quantum Critical Point in $\text{A}_2\text{Cr}_3\text{As}_3$, *Phys. Rev. Lett.* **123**, 047001 (2019).

- [37] D. T. Adroja, A. Bhattacharyya, M. Telling, Y. Feng, M. Smidman, B. Pan, J. Zhao, A. D. Hillier, F. L. Pratt, and A. M. Strydom, Superconducting ground state of quasi-one-dimensional $\text{K}_2\text{Cr}_3\text{As}_3$ investigated using μSR measurements, *Phys. Rev. B* **92**, 134505 (2015).
- [38] Liu, Y. and Bao, J.-K. and Zuo, H.-K. and Ablimit, A. and Tang, Z.-T. and Feng, C.-M. and Zhu, Z.-W. and Cao, G.-H., Effect of impurity scattering on superconductivity in $\text{K}_2\text{Cr}_3\text{As}_3$, *Sci. China: Phys., Mech. Astron.* **59**, 657402 (2016).
- [39] H. Zuo, J.-K. Bao, Y. Liu, J. Wang, Z. Jin, Z. Xia, L. Li, Z. Xu, J. Kang, Z. Zhu, and G.-H. Cao, Temperature and angular dependence of the upper critical field in $\text{K}_2\text{Cr}_3\text{As}_3$, *Phys. Rev. B* **95**, 014502 (2017).
- [40] H. Zhi, T. Imai, F. L. Ning, J.-K. Bao, and G.-H. Cao, NMR Investigation of the Quasi-One-Dimensional Superconductor $\text{K}_2\text{Cr}_3\text{As}_3$, *Phys. Rev. Lett.* **114**, 147004 (2015).
- [41] X.-X. Wu, F. Yang, C. Le, H. Fan, and J.-P. Hu, Triplet p_z -wave pairing in quasi-one-dimensional $\text{A}_2\text{Cr}_3\text{As}_3$ superconductor, *Phys. Rev. B* **92**, 104511 (2015).
- [42] H. Zhong, X.-Y. Feng, H. Chen, and J. Dai, Formation of Molecular-Orbital Bands in a Twisted Hubbard Tube: Implications for Unconventional Superconductivity in $\text{K}_2\text{Cr}_3\text{As}_3$, *Phys. Rev. Lett.* **115**, 227001 (2015).
- [43] L.-D. Zhang, X.-X. Wu, H. Fan, F. Yang, and J.-P. Hu, Revisitation of superconductivity in $\text{K}_2\text{Cr}_3\text{As}_3$ based on the six-band model, *EPL* **113**, 37003 (2016).
- [44] C. Xu, N. Wu, G.-X. Zhi, B.-H. Lei, X. Duan, F. Ning, C. Cao, and Q. Chen, Coexistence of nontrivial topological properties and strong ferromagnetic fluctuations in quasi-one-dimensional $\text{A}_2\text{Cr}_3\text{As}_3$, *Npj Comput. Mater.* **6**, 1 (2020).
- [45] S.-Q. Wu, C. Cao, and G.-H. Cao, Lifshitz transition and nontrivial H-doping effect in the Cr-based superconductor $\text{KCr}_3\text{As}_3\text{H}_x$, *Phys. Rev. B* **100**, 155108 (2019).
- [46] G. Cuono, F. Forte, A. Romano, X. Ming, J. Luo, C. Autieri, and C. Noce, Intrachain collinear magnetism and interchain magnetic phases in Cr_3As_3 —K-based materials, *Phys. Rev. B* **103**, 214406 (2021).
- [47] K. M. Taddei, Q. Zheng, A. S. Sefat, and C. de la Cruz, Coupling of structure to magnetic and superconducting orders in quasi-one-dimensional $\text{K}_2\text{Cr}_3\text{As}_3$, *Phys. Rev. B* **96**, 180506 (2017).
- [48] C. Cao, H. Jiang, X.-Y. Feng, and J. Dai, Reduced dimensionality and magnetic frustration in KCr_3As_3 , *Phys. Rev. B* **92**, 235107 (2015).
- [49] A. Subedi, Strong-coupling electron-phonon superconductivity in noncentrosymmetric quasi-one-dimensional $\text{k}_2\text{cr}_3\text{as}_3$, *Phys. Rev. B* **92**, 174501 (2015).
- [50] Lei, Bing-Hua and Singh, David J., Multigap electron-phonon superconductivity in the quasi-one-dimensional pnictide $\text{K}_2\text{Mo}_3\text{As}_3$, *Phys. Rev. B* **103**, 094512 (2021).
- [51] S. Calder, K. An, R. Boehler, C. Dela Cruz, M. Frontzek, M. Guthrie, B. Haberl, A. Huq, S. A. Kimber, J. Liu, *et al.*, A suite-level review of the neutron powder diffraction instruments at oak ridge national laboratory, *Review of Scientific Instruments* **89**, 092701 (2018).
- [52] J. Rodríguez-Carvajal, Recent advances in magnetic structure determination by neutron powder diffraction, *Physica B: Condensed Matter* **192**, 55 (1993).
- [53] J. P. Perdew, K. Burke, and M. Ernzerhof, Generalized gradient approximation made simple, *Phys. Rev. Lett.* **77**, 3865 (1996).
- [54] D. Singh and L. Nordström, *Planewaves, Pseudopotentials and the LAPW Method*, 2nd ed. ed. (Springer, Berlin, 2006).
- [55] P. Blaha, K. Schwarz, F. Tran, R. Laskowski, G. K. H. Madsen, and L. D. Marks, Wien2k: An apw+lo program for calculating the properties of solids, *J. Chem. Phys.* **152**, 074101 (2020), <https://doi.org/10.1063/1.5143061>.
- [56] See Supplemental Material at [] for details pertaining to: sample synthesis, diffraction data collection, Rietveld refinements and a more indepth discussion of the DFT results.
- [57] I. Zaliznyak and S. Lee, Magnetic neutron scattering, *Spins* (2004).
- [58] L. M. Whitt, T. C. Douglas, S. Chi, K. M. Taddei, and J. M. Allred, A magnetic excitation linking quasi-1d chevreel-type selenide and arsenide superconductors, *arXiv preprint arXiv:2110.10226* (2021).
- [59] H. Zhi, D. Lee, T. Imai, Z. Tang, Y. Liu, and G. Cao, ^{133}Cs and ^{75}As NMR investigation of the normal metallic state of quasi-one-dimensional $\text{Cs}_2\text{Cr}_3\text{As}_3$, *Phys. Rev. B* **93**, 174508 (2016).
- [60] M. C. Rahn, R. A. Ewings, S. J. Sedlmaier, S. J. Clarke, and A. T. Boothroyd, Strong $(\pi, 0)$ spin fluctuations in β -FeSe observed by neutron spectroscopy, *Physical Review B* **91**, 180501 (2015).
- [61] A. E. Taylor, M. J. Pitcher, R. A. Ewings, T. G. Perring, S. J. Clarke, and A. T. Boothroyd, Antiferromagnetic spin fluctuations in LiFeAs observed by neutron scattering, *Physical Review B* **83**, 220514 (2011).
- [62] Z. Wang, W. Yi, Q. Wu, V. A. Sidorov, J. Bao, Z. Tang, J. Guo, Y. Zhou, S. Zhang, H. Li, Y. Shi, X. Wu, L. Zhang, K. Yang, A. Li, G. Cao, J. Hu, L. Sun, and Z. Zhao, Correlation between superconductivity and bond angle of CrAs chain in non-centrosymmetric compounds $\text{A}_2\text{Cr}_3\text{As}_3$ ($A = \text{K}, \text{Rb}$), *Sci. Rep.* **6**, 37878 (2016).
- [63] A. D. Christianson, E. A. Goremychkin, R. Osborn, S. Rosenkranz, M. D. Lumsden, C. D. Malliakas, I. S. Todorov, H. Claus, D. Y. Chung, M. G. Kanatzidis, R. I. Bewley, and T. G. G. Guidi, Unconventional superconductivity in $\text{Ba}_{0.6}\text{K}_{0.4}\text{Fe}_2\text{As}_2$ from inelastic neutron scattering., *Nature* **456**, 930 (2008).
- [64] G. R. Stewart, Unconventional superconductivity, *Adv. Physics* **66**, 75 (2017).
- [65] T. Mason, G. Aeppli, and H. Mook, Magnetic dynamics of superconducting $\text{La}_{1.86}\text{Sr}_{0.14}\text{CuO}_4$, *Phys. Rev. Lett.* **68**, 1414 (1992).
- [66] T. Dahm, D. Manske, and L. Tewordt, Collective modes in high-temperature superconductors, *Phys. Rev. B* **58**, 12454 (1998).
- [67] P. Dai, H. A. Mook, S. M. Hayden, G. Aeppli, T. G. Perring, R. D. Hunt, and F. Doğan, The magnetic excitation spectrum and thermodynamics of high- T_c superconductors, *Science* **284**, 1344 (1999).
- [68] S. Chi, A. Schneidewind, J. Zhao, L. W. Harriger, L. Li, Y. Luo, G. Cao, Z. Xu, M. Loewenhaupt, J. Hu, and P. Dai, Inelastic Neutron-Scattering Measurements of a Three-Dimensional Spin Resonance in the FeAs-Based $\text{BaFe}_{1.9}\text{Ni}_{0.1}\text{As}_2$ Superconductor, *Phys. Rev. Lett.* **102**, 107006 (2009).
- [69] R. Osborn, S. Rosenkranz, E. Goremychkin, and A. Christianson, Inelastic neutron scattering studies of the spin and lattice dynamics in iron arsenide compounds, *Phys. C: Supercond. Appl.* **469**, 498 (2009).

- [70] J. T. Park, G. Friemel, Y. Li, J.-H. Kim, V. Tsurkan, J. Deisenhofer, H.-A. Krug von Nidda, A. Loidl, A. Ivanov, B. Keimer, and D. S. Inosov, Magnetic Resonant Mode in the Low-Energy Spin-Excitation Spectrum of Superconducting $\text{Rb}_2\text{Fe}_4\text{Se}_5$ Single Crystals, *Phys. Rev. Lett.* **107**, 177005 (2011).
- [71] N. Qureshi, P. Steffens, Y. Drees, A. C. Komarek, D. Lamago, Y. Sidis, L. Harnagea, H.-J. Grafe, S. Wurmehl, B. Büchner, and M. Braden, Inelastic Neutron-Scattering Measurements of Incommensurate Magnetic Excitations on Superconducting LiFeAs Single Crystals, *Phys. Rev. Lett.* **108**, 117001 (2012).
- [72] D. J. Scalapino, A common thread: The pairing interaction for unconventional superconductors, *Rev. Mod. Phys.* **84**, 1383 (2012).
- [73] C. Zhang, R. Yu, Y. Su, Y. Song, M. Wang, G. Tan, T. Egami, J. A. Fernandez-Baca, E. Faulhaber, Q. Si, and P. Dai, Measurement of a Double Neutron-Spin Resonance and an Anisotropic Energy Gap for Underdoped Superconducting $\text{NaFe}_{0.985}\text{Co}_{0.015}\text{As}$ Using Inelastic Neutron Scattering, *Phys. Rev. Lett.* **111**, 207002 (2013).
- [74] J. M. Tranquada, G. Xu, and I. A. Zaliznyak, Superconductivity, antiferromagnetism, and neutron scattering, *J. Magn. Mater.* **350**, 148 (2014).
- [75] Q. Wang, Y. Shen, B. Pan, Y. Hao, M. Ma, F. Zhou, P. Steffens, K. Schmalzl, T. Forrest, M. Abdel-Hafiez, *et al.*, Strong interplay between stripe spin fluctuations, nematicity and superconductivity in FeSe , *Nat. Mater.* **15**, 159 (2016).
- [76] T. Xie, D. Gong, H. Ghosh, A. Ghosh, M. Soda, T. Masuda, S. Itoh, F. Bourdarot, L.-P. Regnault, S. Danilkin, *et al.*, Neutron spin resonance in the 112-type iron-based superconductor, *Phys. Rev. Lett.* **120**, 137001 (2018).
- [77] S. Kunkemöller, P. Steffens, P. Link, Y. Sidis, Z. Q. Mao, Y. Maeno, and M. Braden, Absence of a Large Superconductivity-Induced Gap in Magnetic Fluctuations of Sr_2RuO_4 , *Phys. Rev. Lett.* **118**, 147002 (2017).
- [78] K. Taddei, G. Xing, J. Sun, Y. Fu, Y. Li, Q. Zheng, A. Sefat, D. Singh, and C. de la Cruz, Frustrated Structural Instability in Superconducting Quasi-One-Dimensional $\text{K}_2\text{Cr}_3\text{As}_3$, *Phys. Rev. Lett.* **121**, 187002 (2018).
- [79] G. Xing, L. Shang, Y. Fu, W. Ren, X. Fan, W. Zheng, and D. J. Singh, Structural instability and magnetism of superconducting KCr_3As_3 , *Phys. Rev. B* **99**, 174508 (2019).
- [80] P. Alemany and E. Canadell, Links between the Crystal and Electronic Structure in the New Family of Unconventional Superconductors $\text{A}_2\text{Cr}_3\text{As}_3$ ($\text{A} = \text{K}, \text{Rb}, \text{Cs}$), *Inorg. Chem.* **54**, 8029 (2015).
- [81] H. Jiang, G. Cao, and C. Cao, Electronic structure of quasi-one-dimensional superconductor $\text{K}_2\text{Cr}_3\text{As}_3$ from first-principles calculations, *Sci. Rep.* **5**, 16054 (2015).
- [82] Y. Yang, S.-Q. Feng, H.-Y. Lu, W.-S. Wang, and Z.-P. Chen, Electronic Structures of Newly Discovered Quasi-One-Dimensional Superconductors $\text{A}_2\text{Mo}_3\text{As}_3$ ($\text{A} = \text{K}, \text{Rb}, \text{Cs}$), *J. Supercond. Nov. Magn.* **32**, 2421 (2019).
- [83] L.-D. Zhang, X. Zhang, J.-J. Hao, W. Huang, and F. Yang, Singlet s^\pm -wave pairing in quasi-one-dimensional ACr_3As_3 ($\text{A} = \text{K}, \text{Rb}, \text{Cs}$) superconductors, *Phys. Rev. B* **99**, 094511 (2019).
- [84] J. P. Lu, Q. Si, J. H. Kim, and K. Levin, Nmr relaxation and neutron scattering in a fermi-liquid picture of the metallic copper oxides, *Phys. Rev. Lett.* **65**, 2466 (1990).
- [85] G. Wang, Y. Qian, G. Xu, X. Dai, and Z. Fang, Gutzwiller Density Functional Studies of FeAs-Based Superconductors: Structure Optimization and Evidence for a Three-Dimensional Fermi Surface, *Phys. Rev. Lett.* **104**, 047002 (2010).
- [86] J. Yang, Z. T. Tang, G. H. Cao, and G.-q. Zheng, Ferromagnetic Spin Fluctuation and Unconventional Superconductivity in $\text{Rb}_2\text{Cr}_3\text{As}_3$ Revealed by ^{75}As NMR and NQR, *Phys. Rev. Lett.* **115**, 147002 (2015).
- [87] Ž. Gosar, N. Janša, T. Arh, P. Jeglič, M. Klanjšek, H. Zhai, B. Lv, and D. Arčon, Superconductivity in the regime of attractive interactions in the tomonaga-luttinger liquid, *Phys. Rev. B* **101**, 220508 (2020).
- [88] I. I. Mazin and D. J. Singh, Ferromagnetic Spin Fluctuation Induced Superconductivity in Sr_2RuO_4 , *Phys. Rev. Lett.* **79**, 733 (1997).
- [89] M. Sigrist, Introduction to unconventional superconductivity, in *AIP Conference Proceedings*, Vol. 789 (American Institute of Physics, 2005) pp. 165–243.
- [90] X.-X. Wu, C.-C. Le, J. Yuan, H. Fan, and J.-P. Hu, Magnetism in Quasi-One-Dimensional $\text{A}_2\text{Cr}_3\text{As}_3$ ($\text{A}=\text{K}, \text{Rb}$) Superconductors, *Chin. Phys. Lett.* **32**, 057401 (2015).
- [91] C.-C. Liu, C. Lu, L.-D. Zhang, X. Wu, C. Fang, and F. Yang, Intrinsic topological superconductivity with exactly flat surface bands in the quasi-one-dimensional $\text{A}_2\text{Cr}_3\text{As}_3$ ($\text{A}=\text{Na}, \text{K}, \text{Rb}, \text{Cs}$) superconductors, *Phys. Rev. Research* **2**, 033050 (2020).
- [92] J. Yang, J. Luo, C. Yi, Y. Shi, Y. Zhou, and G. qing Zheng, Spin-triplet superconductivity in $\text{K}_2\text{Cr}_3\text{As}_3$, *Science Advances* **7**, eabl4432 (2021), <https://www.science.org/doi/pdf/10.1126/sciadv.abl4432>.